Eur J Nucl Med Mol Imaging (2015) 42:1601–1611
DOI 10.1007/s00259-015-3054-1

ORIGINAL ARTICLE

Alterations of left ventricular deformation and cardiac sympathetic derangement in patients with systolic heart failure: a 3D speckle tracking echocardiography and cardiac ^{123}I-MIBG study

Dario Leosco[1] · Valentina Parisi[1] · Teresa Pellegrino[2,3] · Gennaro Pagano[1] · Grazia Daniela Femminella[1] · Agnese Bevilacqua[1] · Stefania Paolillo[3,4] · Roberto Formisano[1] · Gaetana Ferro[1] · Claudio de Lucia[1] · Maria Prastaro[3] · Pasquale Perrone Filardi[3] · Alberto Cuocolo[3] · Giuseppe Rengo[1,5] · Nicola Ferrara[1]

Received: 21 January 2015 / Accepted: 19 March 2015 / Published online: 7 May 2015

Abstract
Purpose Myocardial contractile function is under the control of cardiac sympathetic activity. Three-dimensional speckle tracking echocardiography (3D-STE) and cardiac imaging with ^{123}I-metaiodobenzylguanidine (^{123}I-MIBG) are two sophisticated techniques for the assessment of left ventricular (LV) deformation and sympathetic innervation, respectively, which offer important prognostic information in patients with heart failure (HF). The purpose of this investigation was to explore, in patients with systolic HF, the relationship between LV deformation assessed by 3D-STE and cardiac sympathetic derangement evaluated by ^{123}I-MIBG imaging.

Methods We prospectively studied 75 patients with systolic HF. All patients underwent a 3D-STE study (longitudinal, circumferential, area and radial) and ^{123}I-MIBG planar and SPECT cardiac imaging.

Results 3D-STE longitudinal, circumferential and area strain values were correlated with ^{123}I-MIBG late heart to mediastinum (H/M) ratio and late SPECT total defect score. After stratification of the patients according to ischaemic or nonischaemic HF aetiology, we observed a good correlation of all 3D-STE measurements with late H/M ratio and SPECT data in the ischaemic group, but in patients with HF of nonischaemic aetiology, no correlation was found between LV deformation and cardiac sympathetic activity. At the regional level, the strongest correlation between LV deformation and adrenergic innervation was found for the left anterior descending coronary artery distribution territory for all four 3D-STE values. In multivariate linear regression analyses, including age, gender, LV ejection fraction, NYHA class, body mass index, heart rate and HF aetiology, only 3D-STE area and radial strain values significantly predicted cardiac sympathetic derangement on ^{123}I-MIBG late SPECT.

Conclusion This study indicated that 3D-STE measurements are correlated with ^{123}I-MIBG planar and SPECT data. Furthermore, 3D-STE area and radial strain values, but not LVEF, predict cardiac sympathetic derangement in human postischaemic HF.

Keywords Left ventricular deformation · Cardiac sympathetic derangement · 3D-Speckle Tracking Echocardiography · ^{123}I-MIBG cardiac imaging · ^{123}I-MIBG SPECT · ^{123}I-MIBG planar imaging

Dario Leosco and Valentina Parisi contributed equally to this work.

Electronic supplementary material The online version of this article (doi:10.1007/s00259-015-3054-1) contains supplementary material, which is available to authorized users.

✉ Giuseppe Rengo
giuseppe.rengo@unina.it

[1] Department of Translational Medical Science, University Federico II, Via S. Pansini 5, 80131 Naples, Italy

[2] Institute of Biostructure and Bioimaging, Italian National Research Council (CNR), Naples, Italy

[3] Department of Advanced Biomedical Science, University Federico II, Naples, Italy

[4] Institute of Diagnostic and Nuclear Development, SDN Foundation, Naples, Italy

[5] IRCCS, Istituto di Telese, Salvatore Maugeri Foundation, Benevento, BN, Italy

Introduction

Sympathetic nervous system (SNS) hyperactivity is a specific compensatory feature of chronic heart failure (HF) [1–3] that activates compensatory responses aimed at enhancing cardiac contractility and preserving cardiac output. However, compelling evidence indicates that, in the long term, SNS overdrive becomes detrimental to the failing heart inducing several molecular abnormalities, including cardiac β-adrenergic receptor downregulation and desensitization that are crucial phenomena contributing to left ventricular (LV) dysfunction, worsening symptoms and increased mortality [1–6]. Cardiac imaging with ^{123}I-metaiodobenzylguanidine (^{123}I-MIBG), an analogue of norepinephrine, allows noninvasive assessment of SNS activity, and decreased ^{123}I-MIBG cardiac uptake, reflecting prolonged sympathetic overactivity, has been observed in patients with HF [7–9]. Reduced ^{123}I-MIBG uptake predicts cardiac death, life-threatening arrhythmias and HF progression, with a prognostic value additional to that of LV dysfunction and neurohormonal activation [7, 8].

In the last few years, three-dimensional speckle tracking echocardiography (3D-STE) has been introduced as a valuable diagnostic tool that allows quantification of myocardial deformation in all three spatial dimensions [10, 11]. This new echocardiographic method accurately assesses LV function and overcomes the limitations inherent in the evaluation of myocardial performance by two-dimensional (2D) LV ejection fraction (LVEF) that is mainly dependent on loading conditions and geometric assumptions. Furthermore, it has recently been reported that cardiac strain imaging is able to detect abnormalities of systolic function in patients with preserved LVEF [10].

Although sympathetic myocardial denervation has been reported to correlate with the severity of cardiac perfusion defects and LV dyssynchrony [11], the relationship between cardiac sympathetic status and LV deformation in HF patients has never been investigated. Thus, the aim of the present study was to investigate the relationship between LV deformation and cardiac sympathetic innervation in patients with chronic systolic HF.

Materials and methods

Study population

The patient population comprised 75 consecutive patients with HF of ischaemic and nonischaemic aetiology enrolled between January 2013 and March 2014 at the Division of Cardiology of University Federico II of Naples. All patients were clinically referred for implantable cardioverter defibrillator (ICD) implantation based on poor LV function without previous life-threatening ventricular arrhythmias (primary prevention) or with prior life-threatening ventricular arrhythmias (secondary prevention). Prior to ICD implantation and within 7 days of enrolment, patients underwent ^{123}I-MIBG planar and SPECT imaging and 3D-STE. Additional inclusion criteria were: (1) LVEF ≤50 %, (2) stable haemodynamic conditions, and (3) no acute coronary syndromes in the previous 6 months. Exclusion criteria were haemodynamic instability, moderate to severe valvular disease, presence of atrial fibrillation and/or flutter, ventricular paced rhythm, myocardial inflammatory disease, and suboptimal echocardiographic image quality.

At the time of enrolment, all subjects underwent a complete clinical examination and blood draw for routine biochemical determinations. Demographic data including age, sex, HF medications, cardiovascular disease risk factors and presence of comorbidities were also collected. The study was approved by the local ethics committee. All procedures performed in the study were in accordance with the ethical standards of the institutional and/or national research committee and with the principles of the 1964 Declaration of Helsinki and its later amendments or comparable ethical standards and conformed to the principles of the Declaration of Helsinki on human research. All patients included in the study gave written informed consent after receiving an detailed explanation of the study protocol and of the potential risks related to the procedures adopted in the study.

3D-STE

Echocardiographic studies were performed using a Vivid E9 ultrasound machine (GE Vingmed Ultrasound, Horten, Norway). A conventional 2D echocardiographic and Doppler study was performed and 2D LVEF was derived from LV volumes calculated by the modified Simpson's method using the apical four-chamber and two-chamber views. A six-beat full-volume 3D LV dataset was acquired in all subjects, taking care to avoid any artefacts and to include all LV segments. 3D-STE strain analysis was conducted using semiautomatic LV quantification. The apical views and the were manually aligned and two reference points were placed in the mitral annular plane and at the apex, at end-diastole and end-systole. After automatic detection of the epicardial border, manual adjustments were performed if necessary to delineate the region of interest (ROI) for the analysis of end-systolic 3D-STE longitudinal, circumferential, radial and area strains. 3D-STE global longitudinal, circumferential, radial and area strains were calculated by averaging the end-systolic segmental values of 17 LV segments using the standardized LV segmentation model. When three or more of the 17 LV segments were excluded for technical reasons, the global strain value was not calculated and the patient was excluded from the study.

All echocardiographic measurements were performed in triplicate by two independent expert echocardiographers

who worked separately and used a dedicated offline software package (Echopac; GE Vingmed Ultrasound). We also utilized for comparison a population of 30 normal controls of similar age and gender distribution as our HF population screened using the echocardiographic and clinical database of our Institution. Normal LV size and geometry, normal LVEF (>55 %), normal left atrial volume index (<29 mL/m^2) and the presence of normal structure and function of the four cardiac valves identified normal echocardiograms. In these control subjects, we excluded the presence of cardiovascular disease (stroke, coronary artery disease, myocardial infarction (MI), revascularization, HF, arrhythmia, peripheral artery disease), cardiovascular disease risk factors (hypertension, diabetes, hyperlipidaemia, smoking), pulmonary or renal disease, systemic disease or any drug therapy.

^{123}I-MIBG myocardial scintigraphy

All patients underwent ^{123}I-MIBG planar and SPECT cardiac imaging according to the recommendations of the EANM Cardiovascular Committee and the European Council of Nuclear Cardiology [12], as previously described in detail [13]. An activity of 111 MBq ^{123}I-MIBG (Covidien, Mallinckrodt) was intravenously administered over 1 to 2 min after thyroid blockade by oral administration of 300 mg potassium perchlorate. Standard anterior 10-min planar images of the thorax (256×256 matrix) were obtained 15 min ("early" images) and 3 h and 50 min ("late" images) after tracer administration. A SPECT study (step and shoot mode, 90 projections, imaging time 30 min, 64×64 matrix) was performed 4 h after tracer administration. Imaging was performed using a dual-head camera system (Skylight; Philips) equipped with a low-energy parallel-hole high-resolution collimator, and the camera peaked at 159 keV with a symmetrical 20 % energy window. The heart to mediastinum (H/M) ratios were computed from early and late planar images by dividing the mean counts per pixel within the myocardium by the mean counts per pixel within the mediastinum. Using dedicated postprocessing software on a dedicated workstation (Philips), the cardiac ROI for assessment was polygonal in shape and drawn manually over the myocardium including the LV cavity on the planar MIBG images. Care was taken to exclude lung and liver from the myocardial ROI. The mediastinal ROI with a square shape was placed on the upper half of the mediastinum and had a size of 7×7 pixels. The location of the mediastinal ROI was determined using as landmarks the lung apex, the upper cardiac border and the medial contours of the lungs.

The MIBG washout rate was calculated using the following formula:

MIBG washout rate = [(early heart counts per pixel − early mediastinum counts per pixel)−(late heart counts per pixel decay-corrected−late mediastinum counts per pixel decay-corrected)]/(early heart counts per pixel−early mediastinum counts per pixel)×100

SPECT studies were processed with filtered back-projection and reconstructed into standard long-axis and short-axis images perpendicular to the heart axis. From SPECT images, defect scores were calculated by assessing the segmental tracer uptake scores using the 17-segment model [14]. Each myocardial segment was scored according to the following tracer uptake scale: *0* normal, *1* mildly reduced, *2* moderately reduced, *3* severely reduced, and *4* no uptake. The total defect score (TDS) was calculated as the sum of the segmental tracer uptake scores (summed score) and separately for each vascular territory. Images were interpreted by consensus of two independent readers. Intraobserver and interobserver reproducibility were excellent, thus confirming our recent results from a low-dose MIBG cardiac imaging protocol in HF patients [13]. No patient was excluded for poor quality of MIBG images.

Statistical analysis

Continuous variables are expressed as means±standard deviation and compared using Student's *t* test (normally distributed) or as medians±interquartile range and compared using the Mann–Whitney *U* test (not normally distributed), as appropriate. The normality of data distributions was evaluated using the Kolmogorov-Smirnov test. Categorical variables are expressed as proportion and compared using the χ^2 test with risk ratios and 95 % confidence intervals quoted. Correlation between variables was assessed by linear regression analysis in the whole population and in the subgroups of patients with ischaemic and nonischaemic HF aetiology. To determine the independent predictors of cardiac sympathetic derangement on ^{123}I-MIBG late SPECT, linear regression analysis was performed and variables achieving $p<0.10$ in univariate analysis, including age, sex, LVEF, NYHA class, body mass index (BMI), heart rate, ischaemic vs. nonischaemic aetiology of HF, diabetes, beta-blocker use, and 3D-STE longitudinal, circumferential, area and radial strain values, were then included in a multivariate analysis according to a four-step method providing the introduction of a single strain for each step. All data were collected in an Excel database and analysed using SPSS version 19.0 (SPSS, Inc., Chicago, IL). Statistical significance was accepted at $p<0.05$.

Results

Demographic and clinical data

The baseline characteristics of the 75 patients included in the study are summarized in Table 1. Their mean age was 64.1± 10.28 years, and the majority of patients were male (86.7 %), and NYHA class II (65.3 %) and III (34.7 %). Mean BMI was 28.6±4.3 kg/m^2. Mean LVEF was 40.8±10 %. An ischaemic aetiology of HF was recognized in 74.7 % of the study population with a large prevalence of previous anterior MI (71.4 %). With regard to common cardiovascular disease risk factors, 34.7 % had a family history of coronary artery disease, 69.3 % had hypertension, 49.3 % had diabetes, 65.3 % were ex-smokers, and 76 % had high cholesterol levels. Chronic obstructive pulmonary disease was seen in 33.3 % of patients, and impaired renal function (glomerular filtration rate <60 ml/min) in 12 %. Rates of therapy with ACE inhibitors, AT1 receptor blockers and beta-blockers were 54.6 %, 28 % and 72 %, respectively.

Table 1 Baseline characteristics of the 75 patients with heart failure

Characteristic	Value
Age (years), mean±SD	64.1±10.28
Male gender, % (*n*)	86.7 (65)
Ischaemic aetiology, % (*n*)	74.7 (56)
LVEF (%), mean±SD	40.8±10
Previous MI, % (*n*)	
Anterior	71.4 (40)
Inferior	25 (14)
Lateral	3.5 (2)
Heart rate (bpm), mean±SD	70.45±11.71
NYHA class, % (*n*)	
II	65.3 (49)
III	34.7 (26)
BMI (kg/m^2), mean±SD	28.6±4.3
Family history of CAD, % (*n*)	34.7 (26)
Hypertension, % (*n*)	69.3 (52)
Diabetes, % (*n*)	49.3 (37)
Smokers, % (*n*)	65.3 (49)
Hypercholesterolaemia, % (*n*)	76 (57)
COPD, % (*n*)	33.3 (25)
GFR <60 ml/mg, % (*n*)	12 (9)
Cardiac drug therapy, % (*n*)	
ACE-I/ARB	82.6 (62)
Beta-blockers	72 (54)
^{123}I-MIBG planar and SPECT data, mean±SD	
Early H/M ratio	1.75±0.21
Late H/M ratio	1.56±0.25
Washout rate	39.6±19.6
Late TDS	35.21±16.96
3D-STE data, mean±SD	
Longitudinal	−7.89±3.18
Circumferential	−8.47±3.72
Area	−14.92±5.69
Radial	19.57±9.26

LVEF left ventricular ejection fraction, *MI* myocardial infarction, *NYHA* New York Heart Association, *BMI* body mass index, *CAD* coronary artery disease, *COPD* chronic obstructive pulmonary disease, *GFR* glomerular filtration rate, *ACE-I* angiotensin-converting enzyme inhibitor, *ARB* angiotensin receptor blocker, *H/M* heart to mediastinum ratio, *TDS* total defect score, *3D-STE* three-dimensional strain echocardiography

MIBG and 3D-STE findings in HF patients

Mean early and late H/M ratios were 1.75±0.21 and 1.56± 0.25, respectively, with a mean washout rate of 39.6±19.6 %. The ^{123}-I MIBG late SPECT mean TDS was 35.21±16.9. 3D-STE longitudinal, circumferential, area and radial strain values were −7.89±3.18, −8.47±3.72, −14.92±5.69 and 19.57± 9.26, respectively. Intraobserver reproducibility for all four 3D-STE parameters was excellent (0.96 for longitudinal, 0.96 for circumferential, 0.95 for area and 0.95 for radial). Similar results were found for interobserver reproducibility (0.95 for longitudinal, 0.94 for circumferential, 0.94 for area and 0.95 for radial).

3D-STE data in HF patients and controls

Significantly reduced 3D-STE global longitudinal, circumferential, area and radial strain values were found in HF patients with respect to controls (p<0.0001; Table 2). 3D-STE measurements in the control group were within the range of values found in a recent study in 265 healthy volunteers using a commercially available GE 3D-STE platform [14]. Importantly, all four 3D-STE strain values demonstrated a highly significant correlation with LVEF in HF patients (Fig. 1).

Relationship between 3D-STE and ^{123}I-MIBG planar and SPECT data

Patients were stratified according to ischaemic or nonischaemic HF aetiology. ^{123}I-MIBG late planar and SPECT parameters were reduced to a similar extent in the two groups (late H/M

Table 2 3D-STE data in heart failure patients and controls

3D-STE parameter	Heart failure patients	Controls	*p* value
Longitudinal	−7.89±3.17	−17.67±2.65	<0.0001
Circumferential	−8.47±3.71	−16.74±2.09	<0.0001
Area	−14.92±5.69	−30.07±4.48	<0.0001
Radial	19.57±9.25	47.02±7.781	<0.0001

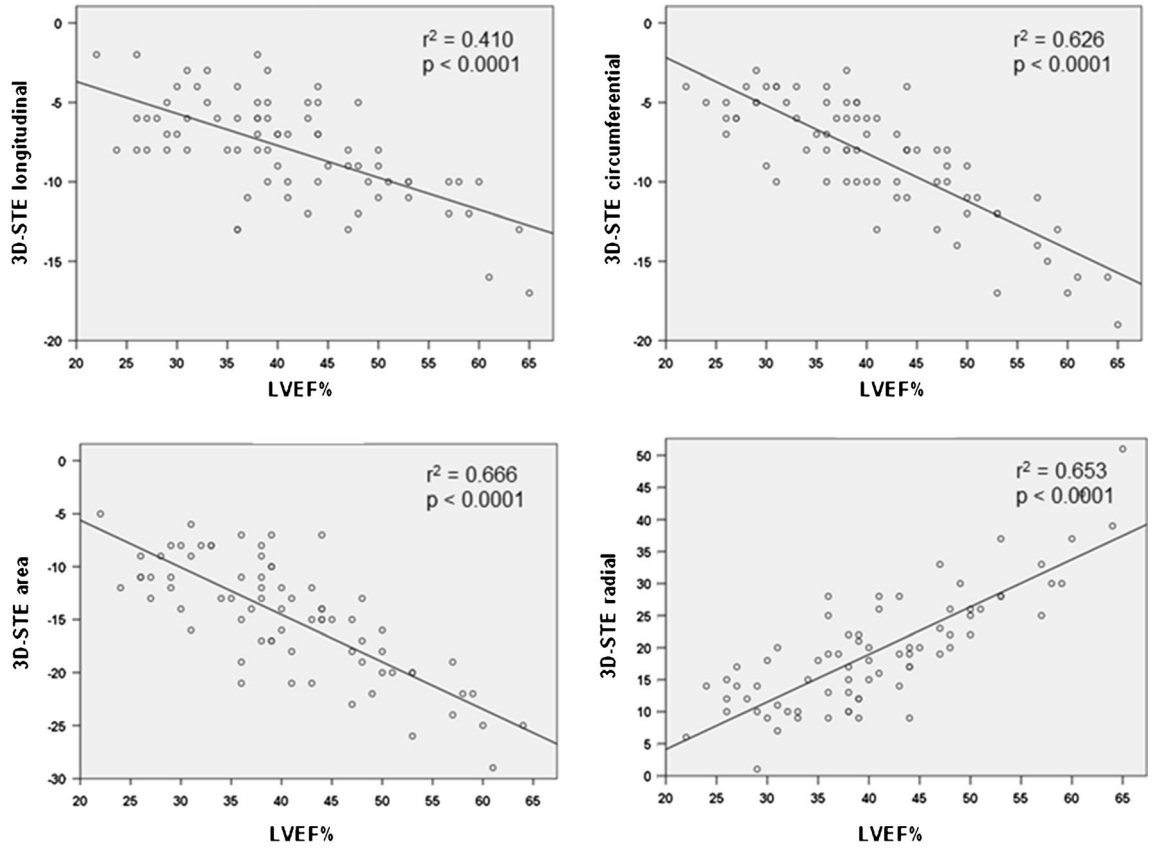

Fig. 1 Correlation between 3D-STE longitudinal, circumferential, area and radial strain values and left ventricular ejection fraction (LVEF) in patients with systolic heart failure

ratio 1.55±0.23 and 1.58±0.27 in the ischaemic and nonischaemic group, respectively, p=NS; SPECT TDS 35.7±16.4 and 33.5±17.8 in the ischaemic vs nonischaemic groups, respectively, p=NS). In the ischaemic group, all 3D-STE values correlated with late H/M ratio and late SPECT data. In patients with HF of nonischaemic aetiology, no correlation was found between LV deformation and ^{123}I-MIBG planar and SPECT data (Table 3). Ischaemic HF patients were further stratified according to the presence of previous anterior MI and previous inferior and/or lateral MI. In both groups, alterations in LV deformation, and signs of cardiac sympathetic nerve damage were also found in myocardial regions remote from those with MI (Supplementary Table 1).

We further explored the regional correlation between 3D-STE and SPECT data according to coronary artery distribution territories. For both 3D-STE and ^{123}I-MIBG SPECT data, the standardized 17-segment model, which assigns

Table 3 Correlation between 3D-STE and ^{123}I-MIBG planar and SPECT data according to HF aetiology

	3D-STE parameter							
	Longitudinal		Circumferential		Area		Radial	
	Pearson coefficient	p value	Pearson coefficient	p value	Pearson coefficient	p value	Pearson coefficient	p value
Ischaemic aetiology								
Late H/M ratio	−0.454	0.000	−0.355	0.007	−0.419	0.001	0.457	0.000
^{123}I-MIBG late SPECT TDS	0.398	0.002	0.459	0.000	0.478	0.000	−0.472	0.000
Nonischaemic aetiology								
Late H/M ratio	−0.197	NS	−0.010	NS	−0.089	NS	0.071	NS
^{123}I-MIBG late SPECT TDS	0.157	NS	−0.011	NS	0.085	NS	−0.097	NS

NS not significant

myocardial segments to the three major coronary arteries, was used [15]. Table 4 indicates that the strongest correlation between LV deformation and innervation was found in the left anterior descending coronary artery (LAD) territory for all four 3D-STE strains considered (Fig. 2). A modest, although significant, correlation continued to be observed for the right coronary artery (RCA) distribution territory limited to 3D-STE circumferential, area, and radial strains. Conversely, no correlation was found between regional echocardiographic and scintigraphic measures in myocardial regions perfused by the left circumflex artery (LCx). Patients with previous anterior MI showed a significant correlation between LV deformation and sympathetic denervation in the LAD distribution territory but not in the myocardial regions served by the LCx and RCA. In contrast, in patients with previous inferior and/or lateral MI, a correlation was also evident in the LAD distribution territory (Supplementary Table 2).

Predictors of cardiac sympathetic derangement on ^{123}I-MIBG late SPECT

Multivariate linear regression analysis was used to analyse the predictors of cardiac sympathetic derangement on ^{123}I-MIBG SPECT (Table 5). A four-step method was used. Step 1 included only 3D-STE longitudinal values along with all factors that were found to be significant in the univariate analysis (age, sex, LVEF, NYHA class, BMI, heart rate, ischaemic vs. nonischaemic aetiology of HF, diabetes, beta-blocker use). Steps 2, 3 and 4 included 3D-STE circumferential, area and radial values, respectively, along with the same variables included in step 1. 3D-STE area and radial values, included in steps 3 and 4, were the only variables that were significantly predictive of ^{123}I-MIBG late SPECT findings. It is noteworthy that LVEF was not significantly predictive of ^{123}I-MIBG late SPECT findings in the linear regression analysis.

Discussion

This study explored the association between LV mechanical deformation, assessed using 3D-STE, and cardiac sympathetic activity, evaluated by ^{123}I-MIBG in patients with systolic HF. We found a correlation between 3D-STE and scintigraphic planar and SPECT data in the whole population. This correlation was found only in the postischaemic HF patients and not in patients with nonischaemic HF. At the regional level, a correlation between LV deformation and sympathetic activity was found for the LAD and RCA distribution territories. Finally, in multivariate analysis, 3D-STE area and radial strain values, but not LVEF, were significant independent predictors of cardiac sympathetic derangement on ^{123}I-MIBG late SPECT.

Table 4 Correlation between 3D-STE and SPECT data according to coronary artery distribution territory

	^{123}I-MIBG late SPECT					
	LAD		LCx		RCA	
	Pearson coefficient	*p* value	Pearson coefficient	*p* value	Pearson coefficient	*p* value
3D-STE longitudinal strain						
LAD	0.448	<0.0001	–	–	–	–
LCx	–	–	0.117	0.318	–	–
RCA	–	–	–	–	0.224	0.053
3D-STE circumferential strain						
LAD	0.336	0.003	–	–	–	–
LCx	–	–	0.190	0.103	–	–
RCA	–	–	–	–	0.266	0.021
3D-STE area strain						
LAD	0.421	<0.0001	–	–	–	–
LCx	–	–	0.217	0.061	–	–
RCA	–	–	–	–	0.303	0.008
3D-STE radial strain						
LAD	−0.408	<0.0001	–	–	–	–
LCx	–	–	−0.223	0.055	–	–
RCA	–	–	–	–	−0.287	0.013

LAD left anterior ascending coronary artery, *LCx* left circumflex coronary artery, *RCA* right coronary artery

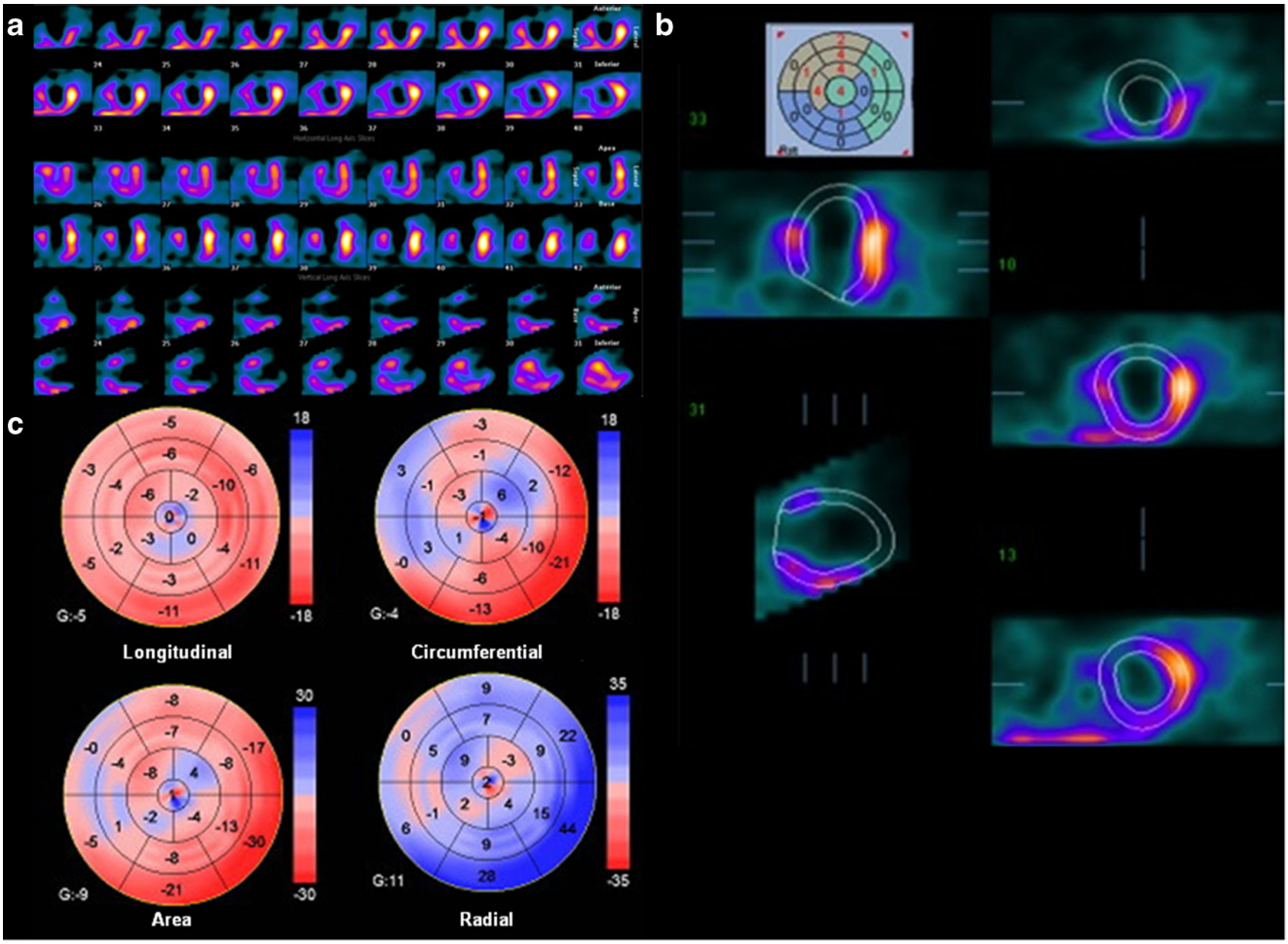

Fig. 2 Representative images of myocardial innervation and left ventricular deformation in a patient with postischaemic heart failure due to previous anteroseptal myocardial infarction. **a**, **b** ^{123}I-MIBG late SPECT slices (**a**, short axis, horizontal and vertical long axis) show a large area of sympathetic denervation in the apical and anteroseptal walls quantified by total defect score (**b**) using the 17-segment model. **c** Longitudinal, circumferential, area and radial 3D-STE images show marked alterations in left ventricular deformation in the anteroseptal regions

3D-STE and cardiac sympathetic derangement in HF patients

Measurement of SNS activity has been suggested to help in the assessment of prognosis and clinical management of HF patients [7, 16]. However, although SNS hyperactivity measured as plasma circulating norepinephrine levels [17–19], cardiac or renal norepinephrine spillover [20], and heart rate variability [21], has a prognostic value in HF patients, none of these approaches is routinely used in clinical practice or recommended by guidelines [22]. In recent years, ^{123}I-MIBG has been proposed as a valuable technique for assessing cardiac adrenergic nerve activity and the H/M ratio has been shown to be an independent predictor of HF progression, arrhythmic cardiac events and cardiac death [7, 8]. However, this scintigraphic technique is not routinely used in HF patients because it is costly, time-consuming and, importantly, unsuitable for close clinical follow-up. A further limitation for developing cardiac innervation imaging in clinical practice is the pharmacological interference of some drugs with MIBG uptake [23]. Thus, identification of more feasible measurements, correlating with ^{123}I-MIBG imaging data would be very useful in HF patients.

In the present study, we found a significant correlation between global and regional LV deformation, as assessed by 3D-STE, and cardiac ^{123}I-MIBG late H/M ratio in a population of patients with systolic HF. Of note, 3D-STE findings were also correlated with ^{123}I-MIBG late SPECT TDS which has recently been shown to be the most powerful independent predictor of ventricular arrhythmias and cardiac death in HF patients with an ICD [24]. Although a correlation between altered cardiac adrenergic tone and LV mechanical dyssynchrony has previously been demonstrated in HF patients [11], an association between cardiac sympathetic activity and LV deformation has never been reported. Our study offers the first demonstration that LV strain in multiple planes is correlated with the state of global and regional LV sympathetic innervation.

Table 5 Multivariate predictors of cardiac sympathetic derangement on ^{123}I-MIBG late SPECT

	Model 1		Model 2		Model 3		Model 4	
	Odds ratio (95 % CI)	*p* value	Odds ratio (95 % CI)	*p* value	Odds ratio (95 % CI)	*p* value	Odds ratio (95 % CI)	*p* value
Age	0.26 (−0.17 – 0.70)	0.22	0.25 (−0.18 – 0.69)	0.25	0.23 (−0.19 – 0.66)	0.27	.24 (−0.18 – 0.67)	0.26
Sex	2.31 (−10.36 – 15.00)	0.71	0.33 (−12.44 – 13.11)	0.95	0.37 (−12.11 – 12.87)	0.95	1.36 (−11.09 – 13.81)	0.82
LVEF	−0.20 (−0.77 – 0.36)	0.47	−0.08 (−0.82 – 0.66)	0.82	0.07 (−0.62 – 0.77)	0.82	.008 (−0.62 – 0.79)	0.80
NYHA	1.38 (−5.56 – 8.33)	0.69	1.23 (−5.74 – 8.21)	0.72	1.50 (−5.35 – 8.35)	0.66	1.28 (−5.57 – 8.14)	0.70
BMI	−0.16 (−1.20 – 0.86)	0.74	−0.16 (−1.20 – 0.87)	0.74	−0.12 (−1.14 – 0.90)	0.81	−0.16 (−1.18 – 0.85)	0.74
Heart rate	0.17 (−0.21 – 0.56)	0.37	0.14 (−0.23 – 0.53)	0.44	0.17 (−0.20 – 0.56)	0.35	0.16 (−0.21 – 0.54)	0.39
Ischaemic/nonischaemic	0.65 (−8.66 – 9.96)	0.89	0.28 (−9.11 – 9.68)	0.95	−0.002 (−9.22 – 9.22)	1.0	−0.18 (−9.42 – 9.06)	0.96
Diabetes	2.36 (−5.47 – 10.20)	0.54	3.17 (−4.76 – 11.11)	0.42	3.00 (−4.74 – 10.75)	0.44	3.49 (−4.30 – 11.28)	0.37
Beta-blocker use	−3.52 (−12.54 – 5.48)	0.43	−5.11(−14.13 – 3.91)	−26	−4.73 (−13.5 – 4.08)	0.28	−4.73 (−13.5 – 4.08)	0.28
3D-STE								
Longitudinal	1,25 (−0.35 – 2.85)	0.12	–	–	–	–	–	–
Circumferential	–	–	1.24 (−0.58 – 3.06)	0.18	–	–	–	–
Area	–	–	–	–	1,14 (0.03 – 2.24)	0.04	–	–
Radial	–	–	–	–	–	–	−0.72 (−1.43 – −0.02)	0.04

LVEF left ventricular ejection fraction, *NYHA* New York Heart Association, *BMI* body mass index

Correlation between 3D-STE and cardiac ^{123}I-MIBG data in patients with HF of ischaemic and nonischaemic aetiology

It is known that significant cardiac sympathetic derangement is evident in patients with systolic HF independently of HF aetiology [7]. In accordance with this, in this study cardiac ^{123}I-MIBG planar and SPECT data were reduced to a comparable extent in patients with HF of ischaemic and nonischaemic aetiology. However, we found an association between LV deformation and cardiac adrenergic activity only in patients with systolic HF of ischaemic aetiology but not in those with nonischaemic HF. Previous studies have demonstrated that sympathetic neuronal damage measured by ^{123}I-MIBG SPECT corresponds to the area of myocardium at risk and that the ^{123}I-MIBG defect is closely correlated with the myocardium at risk in terms of both size and location [25, 26]. However, in the present study, alterations in LV deformation and cardiac sympathetic nerve damage were evident not only at the site of previous MI but also in noninfarcted myocardial areas. Furthermore, MIBG SPECT and 3D-STE findings showed the strongest correlation in the LAD distribution territory in patients with both previous anterior and previous non-anterior MI. In this regard, it is known that sympathetic nerve fibres are more abundant in the anterior wall than in the posterior wall of the LV [27]. Thus, it is reasonable to hypothesize that sympathetic neuronal damage occurring in HF is more easily recognized by MIBG in LV anterior segments even in the absence of necrotic and scar areas.

3D-STE vs. LVEF for the prediction of cardiac ^{123}I-MIBG defect

LV myocardial strain analysis using 3D-STE imaging is able to assess simultaneously LV volumes and function, in combination with the determination of global and regional LV deformation capabilities [28, 29]. Parameters derived from 3D-STE reflect LV contractility in multiple planes and offer the advantage of overcoming the limitations inherent in the assessment of myocardial contractility by LVEF that is mainly dependent on loading conditions and geometric assumptions. Our results indicate a highly significant correlation between all four 3D-STE parameters and LVEF. However, in the multivariate analysis only 3D-STE area and radial strain values, and not LVEF, were independent predictors of cardiac sympathetic derangement on ^{123}I-MIBG SPECT, This is in line with previous results indicating only a modest correlation between cardiac sympathetic innervation and LVEF [7]. Furthermore, no changes in the prognostic impact of ^{123}I-MIBG defects has been observed across a wide range of LVEF values, thus indicating that the assessment of sympathetic myocardial denervation is a more sensitive predictor of a poor prognosis in HF patients with respect to global LV mechanical function, especially in patients with higher LVEF [30]. Our results, demonstrating the independent correlation between 3D-STE area strain value and ^{123}I-MIBG SPECT defects, confirm the value of this parameter for clinical application. It has been validated in vitro and in vivo against reference techniques such as sonomicrometry and MRI [31–35]. Furthermore, 3D-STE area strain value has been shown to predict response to cardiac resynchronization therapy [36].

Previous studies from our group and others have demonstrated that diabetic patients with HF show lower cardiac sympathetic activity than nondiabetic HF patients on MIBG imaging [8, 37, 38]. Moreover, beta-blockers, such as carvedilol and bisoprolol, can increase MIBG uptake in HF patients [39, 40]. However, it is important to emphasize that this improvement does not depend on the direct interference of these drugs with MIBG uptake, but rather on improvement in heart performance and therefore sympathetic tone. In the present study, diabetes and beta-blocker use were not predictive of cardiac sympathetic derangement on ^{123}I-MIBG late SPECT in the multivariate analysis.

Study limitations

We report here a single-centre experience in a relatively small group of patients, and therefore the study needs confirmation in multicentre studies enrolling a larger number of patients. These future studies could also allow investigation of the correlation between MIBG and 3D-STE findings in patients with nonischaemic HF. 3D-STE is a novel method using complex computations; therefore, further validation studies are needed to identify its reliability and feasibility, and to standardize measurements. In this study, we used a low-dose MIBG cardiac imaging protocol. In some patients, lower tracer doses can make the interpretation of MIBG imaging difficult, especially in HF patients with poor quality images. However, we have previously reported good observer reproducibility with this protocol [13], and, in the present study, the quality of the SPECT images was good and interpretation was possible in all patients. Further, it is likely that prior exclusion of patients with poor quality echocardiograms (mostly related to overlying lung) contributed to the selection of subjects with good quality MIBG images. Our study population was at particularly high risk of cardiovascular disease, cautioning the extrapolation of the current findings to the overall HF population. Finally, a mid/long-term follow-up is still not available in our study population, so no conclusions can be drawn as to the potential prognostic value of 3D-STE in HF.

Conclusions

Our study demonstrated for the first time a significant association between LV deformation as evaluated by 3D-STE and ^{123}I-MIBG imaging. Further studies are needed to understand

whether the use of 3D-STE, alone or in combination with ^{123}I-MIBG, could improve prognostic stratification of patients with HF.

Compliance with ethical standards

Conflicts of interest None.

Research involving human participants and/or animals All procedures performed in studies involving human participants were in accordance with the ethical standards of the institutional and/or national research committee and with the principles of the 1964 Declaration of Helsinki and its later amendments or comparable ethical standards.

Informed consent Informed consent was obtained from all individual participants included in the study.

References

1. Triposkiadis F, Karayannis G, Giamouzis G, Skoularigis J, Louridas G, Butler J. The sympathetic nervous system in heart failure physiology, pathophysiology, and clinical implications. J Am Coll Cardiol. 2009;54:1747–62.
2. Lymperopoulos A, Rengo G, Koch WJ. Adrenal adrenoceptors in heart failure: fine tuning cardiac stimulation. Trends Mol Med. 2007;13:503–11.
3. Rengo G, Perrone-Filardi P, Femminella GD, Liccardo D, Zincarelli C, de Lucia C, et al. Targeting the β-adrenergic receptor system through G-protein-coupled receptor kinase 2: a new paradigm for therapy and prognostic evaluation in heart failure: from bench to bedside. Circ Heart Fail. 2012;5:385–91.
4. Rengo G, Lymperopoulos A, Leosco D, Koch WJ. GRK2 as a novel gene therapy target in heart failure. J Mol Cell Cardiol. 2011;50(5):785–92.
5. Iaccarino G, Barbato E, Cipolletta E, De Amicis V, Margulies KB, Leosco D, et al. Elevated myocardial and lymphocyte GRK2 expression and activity in human heart failure. Eur Heart J. 2005;26:1752–8.
6. Leosco D, Rengo G, Iaccarino G, Golino L, Marchese M, Fortunato F, et al. Exercise promotes angiogenesis and improves beta-adrenergic receptor signalling in the post-ischaemic failing rat heart. Cardiovasc Res. 2008;78(2):385–94.
7. Jacobson AF, Senior R, Cerqueira MD, Wong ND, Thomas GS, Lopez VA, et al. ADMIRE-HF Investigators. Myocardial iodine-123 meta-iodobenzylguanidine imaging and cardiac events in heart failure. Results of the prospective ADMIRE-HF (AdreView Myocardial Imaging for Risk Evaluation in Heart Failure) study. J Am Coll Cardiol. 2010;55:2212–21.
8. Paolillo S, Rengo G, Pagano G, Pellegrino T, Savarese G, Femminella GD, et al. Impact of diabetes on cardiac sympathetic innervation in patients with heart failure: a 123I meta-iodobenzylguanidine (123I MIBG) scintigraphic study. Diabetes Care. 2013;36:2395–401.
9. Sood N, Al Badarin F, Parker M, Pullatt R, Jacobson AF, Bateman TM, et al. Resting perfusion MPI-SPECT combined with cardiac 123I-mIBG sympathetic innervation imaging improves prediction of arrhythmic events in non-ischemic cardiomyopathy patients: sub-study from the ADMIRE-HF trial. J Nucl Cardiol. 2013;20:813–20.
10. Kraigher-Krainer E, Shah AM, Gupta DK, Santos A, Claggett B, Pieske B, et al. Impaired systolic function by strain imaging in heart failure with preserved ejection fraction. J Am Coll Cardiol. 2014;63:447–56.
11. Gimelli A, Liga R, Genovesi D, Giorgetti A, Kusch A, Marzullo P. Association between left ventricular regional sympathetic denervation and mechanical dyssynchrony in phase analysis: a cardiac CZT study. Eur J Nucl Med Mol Imaging. 2014;41:946–55.
12. Flotats A, Carrió I, Agostini D, Le Guludec D, Marcassa C, Schäfers M, et al. Proposal for standardization of 123I-metaiodobenzylguanidine (MIBG) cardiac sympathetic imaging by the EANM Cardiovascular Committee and the European Council of Nuclear Cardiology. Eur J Nucl Med Mol Imaging. 2010;37:1802–12.
13. Pellegrino T, Petretta M, De Luca S, Paolillo S, Boemio A, Carotenuto R, et al. Observer reproducibility of results from a low-dose 123I-metaiodobenzylguanidine cardiac imaging protocol in patients with heart failure. Eur J Nucl Med Mol Imaging. 2013;40:1549–57.
14. Muraru D, Cucchini U, Mihăilă S, Miglioranza MH, Aruta P, Cavalli G, et al. Left ventricular myocardial strain by three-dimensional speckle-tracking echocardiography in healthy subjects: reference values and analysis of their physiologic and technical determinants. J Am Soc Echocardiogr. 2014;27:858–871.e1.
15. Cerqueira MD, Weissman NJ, Dilsizian V, Jacobs AK, Kaul S, Laskey WK, et al. Standardized myocardial segmentation and nomenclature for tomographic imaging of the heart. A statement for healthcare professionals from the Cardiac Imaging Committee of the Council on Clinical Cardiology of the American Heart Association. Circulation. 2002;105:539–42.
16. Floras JS. Sympathetic nervous system activation in human heart failure: clinical implications of an updated model. J Am Coll Cardiol. 2009;54:375–85.
17. Latini R, Masson S, Anand I, Salio M, Hester A, Judd D, et al. The comparative prognostic value of plasma neurohormones at baseline in patients with heart failure enrolled in Val-HeFT. Eur Heart J. 2004;25:292–9.
18. Rengo G, Pagano G, Parisi V, Femminella GD, de Lucia C, Liccardo D, et al. Changes of plasma norepinephrine and serum N-terminal pro-brain natriuretic peptide after exercise training predict survival in patients with heart failure. Int J Cardiol. 2014;17:384–9.
19. Rengo G, Galasso G, Femminella GD, Parisi V, Zincarelli C, Pagano G, et al. Reduction of lymphocyte G protein-coupled receptor kinase-2 (GRK2) after exercise training predicts survival in patients with heart failure. Eur J Prev Cardiol. 2014;21:4–11.
20. Tsutamoto T, Nishiyama K, Sakai H, Tanaka T, Fujii M, Yamamoto T, et al. Transcardiac increase in norepinephrine and prognosis in patients with chronic heart failure. Eur J Heart Fail. 2008;10:1208–14.
21. La Rovere MT, Pinna GD, Maestri R, Mortara A, Capomolla S, Febo O, et al. Short-term heart rate variability strongly predicts sudden cardiac death in chronic heart failure patients. Circulation. 2003;4(107):565–70.
22. McMurray JJ, Adamopoulos S, Anker SD, Auricchio A, Böhm M, Dickstein K, et al. ESC guidelines for the diagnosis and treatment of acute and chronic heart failure 2012: The Task Force for the Diagnosis and Treatment of Acute and Chronic Heart Failure 2012 of the European Society of Cardiology. Developed in collaboration with the Heart Failure Association (HFA) of the ESC. Eur J Heart Fail. 2012;14:803–69.
23. Stefanelli A, Treglia G, Bruno I, Rufini V, Giordano A. Pharmacological interference with 123I-metaiodobenzylguanidine: a limitation to developing cardiac innervation imaging in clinical practice? Eur Rev Med Pharmacol Sci. 2013;17:1326–33.
24. Boogers MJ, Borleffs CJ, Henneman MM, van Bommel RJ, van Ramshorst J, Boersma E, et al. Cardiac sympathetic denervation assessed with 123-iodine metaiodobenzylguanidine imaging

predicts ventricular arrhythmias in implantable cardioverter-defibrillator patients. J Am Coll Cardiol. 2010;55:2769–77.
25. Matsunari I, Schricke U, Bengel FM, Haase HU, Barthel P, Schmidt G, et al. Extent of cardiac sympathetic neuronal damage is determined by the area of ischemia in patients with acute coronary syndromes. Circulation. 2000;101:2579–85.
26. Zipes DP. Influence of myocardial ischemia and infarction on autonomic innervation of heart. Circulation. 1990;82:1095–105.
27. Kawano H, Okada R, Yano K. Histological study on the distribution of autonomic nerves in the human heart. Heart Vessel. 2003;18:32–9.
28. Xu TY, Sun JP, Lee AP, Yang XS, Qiao Z, Luo X, et al. Three-dimensional speckle strain echocardiography is more accurate and efficient than 2D strain in the evaluation of left ventricular function. Int J Cardiol. 2014;176:360–6.
29. Badano LP, Cucchini U, Muraru D, Al Nono O, Sarais C, Iliceto S. Use of three-dimensional speckle tracking to assess left ventricular myocardial mechanics: inter-vendor consistency and reproducibility of strain measurements. Eur Heart J Cardiovasc Imaging. 2013;14(3):285–93.
30. Shah AM, Bourgoun M, Narula J, Jacobson AF, Solomon SD. Influence of ejection fraction on the prognostic value of sympathetic innervation imaging with iodine-123 MIBG in heart failure. JACC Cardiovasc Imaging. 2012;5:1139–46.
31. Pérez de Isla L, Balcones DV, Fernández-Golfín C, Marcos-Alberca P, Almería C, Rodrigo JL, et al. Three-dimensional-wall motion tracking: a new and faster tool for myocardial strain assessment: comparison with two-dimensional-wall motion tracking. J Am Soc Echocardiogr. 2009;22:325–30.
32. Nesser HJ, Mor-Avi V, Gorissen W, Weinert L, Steringer-Mascherbauer R, Niel J, et al. Quantification of left ventricular volumes using three-dimensional echocardiographic speckle tracking: comparison with MRI. Eur Heart J. 2009;30:1565–73.
33. Saito K, Okura H, Watanabe N, Hayashida A, Obase K, Imai K, et al. Comprehensive evaluation of left ventricular strain using speckle tracking echocardiography in normal adults: comparison of three-dimensional and two-dimensional approaches. J Am Soc Echocardiogr. 2009;22:1025–30.
34. Zhou Z, Ashraf M, Hu D, Dai X, Xu Y, Kenny B, et al. Three-dimensional speckle-tracking imaging for left ventricular rotation measurement: an in vitro validation study. J Ultrasound Med. 2010;29:903–9.
35. Seo Y, Ishizu T, Enomoto Y, Sugimori H, Yamamoto M, Machino T, et al. Validation of 3-dimensional speckle tracking imaging to quantify regional myocardial deformation. Circ Cardiovasc Imaging. 2009;2:451–9.
36. Tatsumi K, Tanaka H, Tsuji T, Kaneko A, Ryo K, Yamawaki K, et al. Strain dyssynchrony index determined by three dimensional speckle area tracking can predict response to cardiac resynchronization therapy. Cardiovasc Ultrasound. 2011;9:11. doi: 10.1186/1476-7120-9-11.
37. Gerson MC, Caldwell JH, Ananthasubramaniam K, Clements IP, Henzlova MJ, Amanullah A, et al. Influence of diabetes mellitus on prognostic utility of imaging of myocardial sympathetic innervation in heart failure patients. Circ Cardiovasc Imaging. 2011;4:87–93.
38. Paolillo S, Rengo G, Pellegrino T, Formisano R, Pagano G, Gargiulo P, et al. Insulin resistance is associated with impaired cardiac sympathetic innervation in patients with heart failure. Eur Heart J Cardiovasc Imaging. 2015. doi:10.1093/ehjci/jev061.
39. Cohen-Solal A, Rouzet F, Berdeaux A, Le Guludec D, Abergel E, Syrota A, et al. Effects of carvedilol on myocardial sympathetic innervation in patients with chronic heart failure. J Nucl Med. 2005;46:1796–803.
40. Lotze U, Kaepplinger S, Kober A, Richartz BM, Gottschild D, Figulla HR. Recovery of the cardiac adrenergic nervous system after long-term beta-blocker therapy in idiopathic dilated cardiomyopathy: assessment by increase in myocardial 123I-metaiodobenzylguanidine uptake. J Nucl Med. 2001;42:49–54.